Journal of Catalysis **200,** 148–159 (2001)
doi:10.1006/jcat.2001.3185, available online at http://www.idealibrary.com on IDEAL®

Hydrothermal Stabilization by Lanthanum of Mixed Metal Oxides and Noble Metal Catalysts for Volatile Organic Compound Removal

Magali Ferrandon[1] and Emilia Björnbom

Department of Chemical Engineering and Technology, Division of Chemical Reaction Engineering, Royal Institute of Technology, SE-100 44 Stockholm, Sweden

Received October 31, 2000; revised January 10, 2001; accepted January 10, 2001; published online April 18, 2001

Catalysts based on manganese or copper oxides, mixed with platinum or palladium, supported on alumina alone or doped with lanthanum were characterized by BET, XRD, SEM, HRTEM, TPR, and XPS and tested for the oxidation of a mixture of naphthalene, CO, and CH_4 in air, CO_2, and water. The catalysts were also aged at 900°C for 300 h in 10% steam. La was found in a dispersed phase in the alumina washcoat both before and after aging. Fresh manganese oxide catalysts, calcined at 800°C, contained mostly Mn_2O_3, while on fresh copper samples, surface Cu^{2+} species were prevalent. It was found that Mn and Cu were better dispersed onto the alumina washcoat in the presence of La and that La increased the saturation of copper into alumina. The reducibility by H_2 of copper was also lowered by La. After aging, only CuO appeared on the unpromoted Cu-based catalysts, whereas, in the presence of La, the surface Cu^{2+} species were still present. The presence of active phases, particularly Cu and Pd, increased the formation of α-Al_2O_3 and the particle size of the alumina washcoat after aging. More than 60% of CuO reacted with alumina to form the spinel compound, $CuAl_2O_4$, whereas in presence of La, no spinel was formed. The addition of La onto fresh manganese-based catalysts led to an enhancement of the oxidation of CH_4. The CuO–Pd/La–Al_2O_3 catalyst was found to be the most active catalyst for the oxidation of CO, $C_{10}H_8$, and CH_4 before and after aging.

Key Words: **manganese oxides; copper oxide; platinum; palladium; lanthanum; naphthalene; carbon monoxide; methane; oxidation; deactivation; stabilization; sintering; TPR; XPS.**

INTRODUCTION

Increasing the lifetime of catalysts for the removal of volatile organic compounds (VOCs) is one of the biggest challenges of catalyst development today. The deactivation of catalysts falls into four general categories: chemical, fouling, mechanical, and thermal (1), the latter being a more serious problem since it is irreversible. Thermal deactivation of the catalysts may result from sintering of the washcoat and/or the active phases (2). Many important industrial processes are based on high-surface-area (150–200 m^2/g) γ-alumina-supported catalysts. Sintering of γ-alumina may result from several processes, one of which is phase transformation to the thermodynamically stable α-alumina (2). When γ-alumina is transformed to the α state, its specific surface area and pore volume decrease. Moreover, this is accompanied by a decrease in the mechanical strength of the catalyst (3) in addition to its specific volume, creating voids which also lead to an increase in the attrition phenomenon (4).

Since the transformation of the metastable α-phase is irreversible, loss of activity is permanent. Such morphological changes in a catalyst support are accompanied by a loss of activity occasioned by an encapsulation of the active component, known as the "earthquake phenomena" (5). Moreover, thermal sintering of the alumina washcoat may cause a loss of the metal area (crystallite sintering) due to macroscopic movement of the substrate during phase transformation of the alumina (6–8).

On the other hand, it has been observed that metals such as Pt (9–11), as well as oxides of metals such as Mn, Ni, and Cu (12–14), could accelerate the phase transformation of alumina into the stable α form. Metal oxides generally have a stronger effect on the sintering than noble metals do, due to their higher concentration.

The addition of a stabilizer may inhibit the sintering effect. Lanthanum appears to be one of the best additives for inhibiting the sintering of high-surface-area alumina (11, 15, 16), especially when active species are deposited on it (3, 17). Lanthanum is particularly adapted for the reactive atmosphere which contains water (18, 19). Also, it has been reported that the addition of lanthanum into the alumina washcoat increases the dispersion of Pt (20–22) and Pd (23), and it also has an effect on stabilization of the particle size of the metals (24).

Depending on the preparation method and on the treatment conditions used, the optimum concentration of lanthanum to be added into the alumina may vary (18, 20, 25–27). Usually, a low lanthanum content is sufficient to preserve the alumina against thermal sintering at temperatures

[1] To whom correspondence should be addressed. Fax: +46(0) 8 10 85 79, Email: mafe@ket.kth.se.

0021-9517/01 $35.00

below 1050°C (18). However, the amount of lanthanum necessary to ensure such a stabilizing effect depends also on the properties of the starting alumina material (28). A good dispersion of lanthanum throughout the alumina depends on the method used to insert the lanthanum. Compared with other methods studied, the specific adsorption of a $La(EDTA)^-$ complex on alumina has been found to result in supports that were more homogeneously covered with lanthanum (27).

Precious metals are well-known total oxidation catalysts with high activities, and are widely used for controlling exhaust gas emissions. The high cost of precious metals and their sensitivity to high temperatures have long motivated the search for substitute catalysts. Metal oxides are generally less active and stable in the presence of water-vapor and sulfur compounds than the precious-metal catalysts. Our previous works have shown that mixtures of metal oxides (MnO_x and CuO) and small amounts of noble metals (Pt, Pd) have much higher resistance to thermal or sulfur dioxide treatments than single-component catalysts (29).

Many studies have reported on the interaction between lanthanum and alumina, but little information is available on the interaction of lanthanum with the active phases in the washcoat, particularly with the metal oxides.

Combustion of wood has recently gained interest in Europe as an alternative to fossil fuels; however, the combustion emissions contain harmful compounds such as VOCs, CO, and polyaromatics that are now regulated.

The present work deals with the hydrothermal stabilization of catalysts for total oxidation. Catalysts containing combinations of manganese or copper oxides, and low amounts of platinum or palladium, supported on γ-alumina alone or stabilized with 3 mol% lanthanum, were selected for the study. Characterization techniques such as BET, XRD, SEM, TEM, TPR, and XPS were used to study the interactions between lanthanum and the metal oxides in the alumina washcoat. Catalytic activity was evaluated by oxidation of a complex mixture of naphthalene, CO, and methane in the presence of air, CO_2, and water.

EXPERIMENTAL

Preparation of Catalysts

γ-Alumina (Puralox SBA-170, Condea Chemie, Germany, 171 m^2/g) was used as the starting material. The addition of 3 mol% lanthanum onto the alumina was done by specific adsorption of a $La(EDTA)^-$ complex onto the alumina (27). The active components were deposited using the deposition–precipitation method (30). The following eight catalysts were prepared: MnO_x–Pt/Al_2O_3, MnO_x–Pt/La–Al_2O_3, MnO_x–Pd/Al_2O_3, MnO_x–Pd/La–Al_2O_3, CuO–Pt/Al_2O_3, CuO–Pt/La–Al_2O_3, CuO–Pd/Al_2O_3, and CuO–Pd/La–Al_2O_3. Manganese nitrate ($Mn(NO_3)_2 \cdot 4H_2O$, Merck, 98.5%) or copper nitrate ($Cu(NO_3)_2 \cdot 3H_2O$, Merck, 99.5%) and urea (Merck, pro analysi) were added to a suspension of γ-alumina or La-doped alumina. Platinum salt ($Pt(NO_3)_2$, ChemPur, Germany, 50%) or palladium salt ($Pd(NO_3)_2$, ChemPur, Germany, 41%) was then added. The suspension was stirred for several hours at 90°C until a gel was formed. Finally, the slurry was dried overnight at 200°C. The target loadings were 10 mol% Mn and Cu and 0.1 mol% Pt and Pd of the washcoat counted as Al_2O_3.

Several samples of CuO deposited on γ-alumina and La-doped alumina (1.6, 3.2, 4.8, 6.4, and 8 mol%/100 m^2/g Al_2O_3) were prepared by impregnating the washcoat with copper nitrate via the incipient wetness technique. The powders were then dried at 110°C and then calcined at 300°C to minimize the risk of reaction of copper with the washcoat. Commercial samples of CuO (Micromeritics) and $CuAl_2O_4$ (Johnson Matthey Gmbh) were also used.

Monoliths made of cordierite with a cylindrical shape (diameter, 20 mm; height, 25 mm) and a cell density of 400 cpsi were used. The impregnated washcoat powders were dispersed in water and ball-milled overnight. The monoliths were then immersed in the slurry for approximately 5 min. The excess slurry was removed by blowing air through the channels. Several dips, followed by drying at 200°C for a few hours, were needed to obtain a washcoat loading of ca. 20 wt% of the total catalyst weight. Finally, the catalysts were calcined at 800°C for 4 h in air.

Deactivation Treatment

Hydrothermal treatment was performed on the impregnated washcoat powders with active phases and on the monolithic catalysts, using an airflow of 1 l/min with 10% steam, at 900°C for 300 h, for both La-stabilized and undoped alumina. The conditions chosen for this aging process were intended to mimic the high temperatures (up to 900°C) reached in the flue duct of a wood boiler and the presence of steam during a burning cycle.

Characterization

The surface area and the pore volume of the catalysts were determined by nitrogen adsorption using a Micromeritics ASAP 2000, after outgassing the samples in a vacuum at 250°C. The phase compositions of the samples were investigated by powder X-ray diffraction using a Siemens Diffractometer 5000, operating with the following parameters: Cu $K\alpha$ radiation of 30 mA, 40 kV; Ni filter, 2θ scanning range 20–80°; and scan-step size of 0.02. The weight percent of α-Al_2O_3 was determined by comparison of the absolute α-Al_2O_3 intensity of the samples with that of known mixtures of γ-Al_2O_3 and α-Al_2O_3. The crystal particle size of Al_2O_3 was estimated by peak broadening with Scherrer's formula (31). The rough-scale distribution

of lanthanum was assessed by scanning electron microscopy (SEM), using a Zeiss DSM 940 with a resolution of 20–50 Å, combined with element detection (EDX). High-resolution transmission electronic microscopy (HRTEM) with a TOPCON EM002B equipped with EDX (14-nm depth) was used to measure the particle size of the metals and to visualize the homogeneity of their dispersion onto the surface. The resolution of the instrument was 1.8 Å. Temperature-programmed reduction (TPR) analysis was carried out using 5% H_2 in Ar with a flow rate of 40 ml/min in a Micromeritics 2900 instrument equipped with a thermal conductivity detector. The temperature was raised 5°C/min to 700°C. The amount of the samples was 200 ± 2 mg. The values of the operating variables were selected according to Monti *et al.* to avoid artifacts (32). Water produced in the reduction reaction was frozen out using a cold trap filled with a mixture of liquid nitrogen and 2-propanol. Calibration for the hydrogen consumption was carried out by reduction of bulk CuO. X-ray photoelectron spectroscopy (XPS), employing a Kratos XSAM 800 instrument using a magnesium anode (1253.6 eV), was used to determine the distribution of the elements (2-nm depth). Sensitivity factors used in the quantitative analyses were La 3*d* 10.0, Mn 2*p* 2.60, and Cu 2*p* 6.30. The binding energies for all the samples were referenced to the C 1*s* line at 284.6 eV. In order to avoid reduction of copper species during XPS experiments (33), the samples were analyzed using a short acquisition time (15 min).

Activity Measurements

The activity of the catalysts before and after they had been exposed to the hydrothermal treatment was tested for their oxidation of a mixture of carbon monoxide (2550 ppm), naphthalene (50 ppm), and methane (200 ppm) in O_2 (10%), CO_2 (12%), H_2O (12%), and N_2 (balance, 66%). Naphthalene was included because it is a very stable product arising from the pyrolysis of wood and because it constitutes 50% of all the polyaromatics in the flue gases from wood combustion. Methane was included because it is a constituent in exhausts from wood combustion and because it is a very difficult compound to oxidize, in addition to being a potent greenhouse gas. The reactor used was an Inconel tube placed in a tubular furnace. During the activity tests, the temperature of the furnace was increased from 100°C to 800°C at a heating rate of 3°C/min. The total flow of the gas mixture was 2.5 l/min, corresponding to a space velocity of approximately 20,000 h^{-1}, which mimics that of wood boilers. The contents of methane and naphthalene in the leaving gases were determined every 24 s using a gas chromatograph, HP5890, equipped with a flame ionization detector. Carbon monoxide was analyzed by a nondispersive infrared spectrophotometer (NDIR, Rosemount, BINOS 100).

RESULTS AND DISCUSSIONS

The brown colors of the manganese-containing samples, calcined at 800°C for 4 h, were similar and did not change after the hydrothermal treatment at 900°C for 300 h. The copper samples deposited on undoped alumina were green when calcined at 800°C and, after the hydrothermal treatment, turned to a reddish color, which is the color of copper aluminum oxide; however, the samples deposited on La-doped alumina retained their green color.

BET Areas

The specific surface area of alumina doped with lanthanum was slightly smaller than the area of the starting alumina after calcination at 800°C for 4 h (Table 1). This small decrease of the surface area in the presence of the 4% lanthanum could be due to the formation of La compound which has almost no area, leaving the overall BET area of the solid to be made up largely from the 96% alumina. Another probable explanation is that a certain number of the alumina pores could have been plugged, as seen by the lower total pore volume and average pore diameter of La-doped alumina (0.36 cm^3/g and 109 Å) compared to that of pure alumina (0.40 cm^3/g and 115 Å). However, the stabilizing effect of lanthanum was observed after the hydrothermal treatment at 900°C for 300 h (Table 1).

For all the samples containing active phases and calcined at 800°C for 4 h, the surface area was slightly lower for those containing lanthanum. Also, all the samples containing copper had a lower specific surface area than those containing

TABLE 1

Surface Area, α-Al_2O_3 Content, and α-Al_2O_3 Particle Size of the Catalysts (La, 3 mol%/Al_2O_3; Mn, Cu, 10 mol%/Al_2O_3; Pt, Pd, 0.1 mol%/Al_2O_3)

	Surface area (m^2/g)[a]		%α-Al_2O_3,[b]	α-Al_2O_3 particle size (nm),[c]
	Fresh	HT	HT	HT
Al_2O_3	169	97	None	—
La–Al_2O_3	146	110	None	—
MnO_x–Pt/Al_2O_3	156	27	50	70
MnO_x–Pt/La–Al_2O_3	140	86	None	—
MnO_x–Pd/Al_2O_3	149	10	58	100
MnO_x–Pd/La–Al_2O_3	143	96	None	—
CuO–Pt/Al_2O_3	133	15	53	90
CuO–Pt/La–Al_2O_3	120	62	7	—
CuO–Pd/Al_2O_3	131	7	76	100
CuO–Pd/La–Al_2O_3	126	68	5	—

[a] Determined by BET measurements on samples calcined at 800°C for 4 h in air (fresh) and hydrothermally treated at 900°C for 300 h in 10% steam (HT).

[b] Determined by XRD on hydrothermally treated samples.

[c] Determined by XRD from the peak $2\theta = 35.2$ width at half-maximum on hydrothermally treated samples.

manganese or without any active phase. For the samples deposited on undoped alumina, those which contained Pd had slightly lower surface areas than those containing Pt, whereas the opposite was true for samples deposited on La-doped alumina. It is again probable that some of the active components had inserted themselves in the small pores of the support, thereby diminishing their diameter and blocking some of them, thus leading to a decrease in surface area. After hydrothermal treatment at 900°C for 300 h in 10% steam, the samples containing active phases deposited on Al_2O_3 also had a very low surface area (up to 30 m^2/g), in particular, the samples which contained Pd and/or CuO. The difference between the surface area of alumina alone and that of alumina with active phases was much bigger after the aging. For the catalysts containing lanthanum, the surface areas ranged from 60 up to 100 m^2/g after the deactivation treatment.

X-Ray Diffraction

XRD analysis of all the samples containing active phases, calcined at 800°C for 4 h, showed the presence of a mixture of γ-, δ-, and θ-Al_2O_3 phases with undoped alumina containing slightly more θ phase (data not shown).

The results from the XRD analyses of the manganese-containing samples, hydrotreated at 900°C for 300 h, are shown in Fig. 1. The XRD patterns of the samples of MnO_x–Pt/Al_2O_3 and MnO_x–Pd/Al_2O_3 showed high crystallinity while the patterns of the samples of MnO_x–Pt/La–Al_2O_3 and MnO_x–Pd/La–Al_2O_3 were diffuse. XRD analysis of MnO_x–Pt/Al_2O_3 and MnO_x–Pd/Al_2O_3 showed mainly the presence of 50–60% α-Al_2O_3, whereas no α-Al_2O_3 was detected on samples containing lanthanum (Table 1). The crystal particle size for MnO_x–Pt/Al_2O_3 and MnO_x–Pd/Al_2O_3 was around 70 and 100 nm, respectively, as determined by Scherrer's formula (Table 1). It should be noted that while X-ray line broadening measurements are useful as a relative measure of average crystallite size, the Scherrer formula should not be used for absolute determinations.

The results from the XRD analyses of the copper-containing samples, hydrotreated at 900°C for 300 h, are shown in Fig. 2. The XRD patterns of CuO–Pt/Al_2O_3 and CuO–Pd/Al_2O_3 showed the presence of α-Al_2O_3 and some copper aluminate ($CuAl_2O_4$). The pattern of CuO–Pd/Al_2O_3 presented slightly higher peaks than that of CuO–Pt/Al_2O_3, indicating a higher extent of crystallinity in the former, evidenced also by the amount of α-Al_2O_3 in both samples (76 and 53%, respectively). The crystal particle size was around 90–100 nm, as determined by Scherrer's formula, for both CuO–Pt/Al_2O_3 and CuO–Pd/Al_2O_3. The α-Al_2O_3 was present to a smaller extent in the CuO–Pd/La–Al_2O_3 and CuO–Pt/La–Al_2O_3 samples, i.e., 5–7% (Table 1).

The presence of bulk spinel compound after hydrothermal treatment at 900°C was detected only in the copper-containing undoped samples, but not in those containing manganese. According to the phase diagrams, from 800°C onward, copper reacted more readily with alumina to form copper aluminate (34), compared to manganese which formed spinel compounds only from 1000°C onward (35).

Other authors have reported the presence of bulk copper spinel compounds after aging (15, 36). Despite a lower or similar amount of lanthanum and a more severe treatment, the copper-based catalysts prepared in this study did not present any bulk copper aluminate.

Scanning Electronic Microscopy

SEM analysis was done on samples of MnO_x–Pt and CuO–Pt, both deposited on alumina alone and on

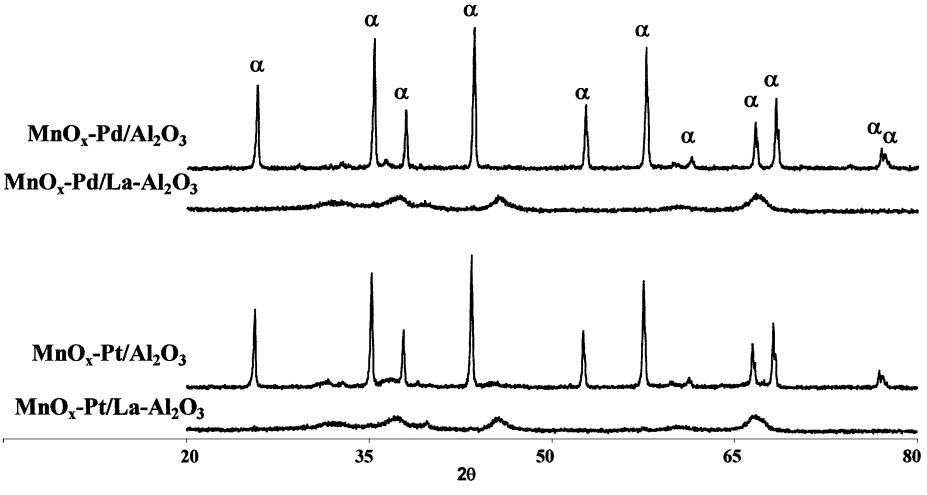

FIG. 1. XRD patterns of MnO_x–Pt and MnO_x–Pd (Mn, 10 mol%/Al_2O_3; Pt, Pd, 0.1 mol%/Al_2O_3) deposited on alumina alone and stabilized with lanthanum (3 mol%/Al_2O_3) after hydrothermal treatment at 900°C for 300 h in 10% steam. α, α-Al_2O_3.

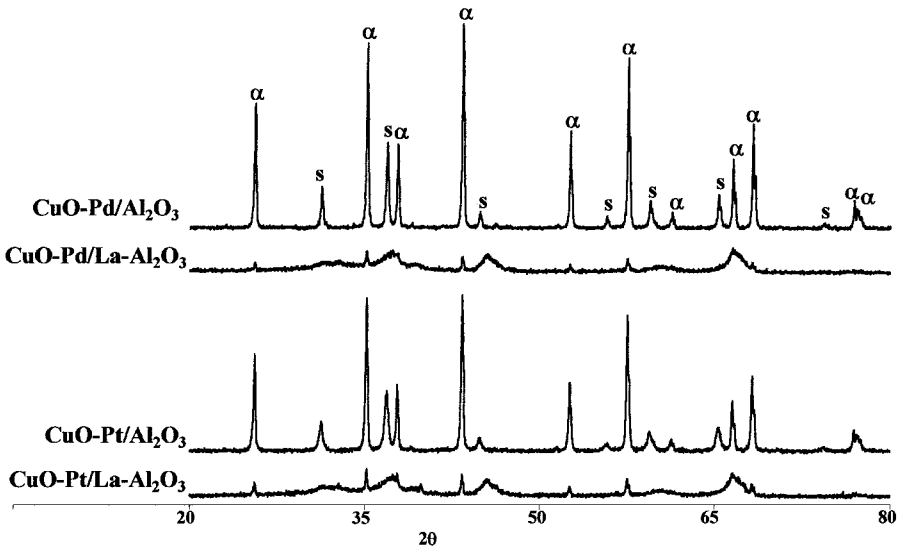

FIG. 2. XRD patterns of CuO–Pt and CuO–Pd (Cu, 10 mol%/Al_2O_3; Pt, Pd, 0.1 mol%/Al_2O_3) deposited on alumina alone and stabilized with lanthanum (3 mol%/Al_2O_3) after hydrothermal treatment at 900°C for 300 h in 10% steam. α, α-Al_2O_3, s, $CuAl_2O_4$.

lanthanum-stabilized alumina, before and after hydrothermal treatment at 900°C for 300 h in steam. The SEM pictures and EDX analysis revealed a good dispersion of the lanthanum on the alumina (data not shown). Pt could not be detected by the EDX analysis. Mn and Cu were better dispersed on fresh alumina containing lanthanum than on those deposited on alumina alone. The differences in the dispersions of the metal oxides were clearer on the samples which had been hydrothermally treated.

High-Resolution Transmission Electronic Microscopy

TEM and HRTEM were performed on MnO_x–Pt/Al_2O_3 and MnO_x–Pt/La–Al_2O_3 samples after hydrothermal treatment (900°C for 300 h). MnO_x–Pt/Al_2O_3 showed a much more crystalline structure than MnO_x–Pt/La–Al_2O_3 (data not shown). The particle size of alumina on MnO_x–Pt/Al_2O_3 was estimated to be between 40 and 100 nm, which was in agreement with the values determined by X-ray line broadening. For the samples containing lanthanum, the alumina appeared more amorphous with smaller grains of less than 10 nm.

As measured by EDX, the atomic ratio of Mn/Al in the doped sample (0.058) was close to the theoretical ratio (0.05), while it was higher in the undoped sample (0.07). This indicated that lanthanum kept the manganese well dispersed on the surface of the alumina, whereas on undoped samples, there was an enrichment of manganese at the surface after aging, due probably to the higher extent of sintering of the washcoat. The ratio of La/Al obtained on the MnO_x–Pt/La–Al_2O_3 sample (0.012) was also very close to the theoretical value (0.015), indicating an effective dispersion of the lanthanum species.

Oudet *et al*. (24) reported that the presence of lanthanum strongly modifies the morphological aspect of the alumina support, which appears poorly crystallized and composed of particles of undefined shape. This provides an increased number of nucleation sites for metals during the first steps of deposition, leading to an enhancement of the initial repartition and dispersion of the metallic phase on the doped samples. The role of lanthanum is also to decrease the movements of the washcoat and thus restrain the coalescence of the metal particles.

Temperature-Programmed Reduction

TPR not only shows the quantity of hydrogen consumed and thus the degree of oxidation of the metal, but also gives information about the species produced during calcination, especially through analysis of the reduction temperature (37), and it further shows the influence of the support on the metal oxides (38, 39). It can also be correlated with the activity for the oxidation of CO (40) or methane (41).

TPR experiments were performed on Pt/Al_2O_3 or Pd/Al_2O_3 (0.1 mol%/Al_2O_3) but no signal was observed in both cases, due probably to the limitation of our instrument.

Manganese Oxide Samples

The profiles of the four samples containing manganese oxides (MnO_x–Pt/Al_2O_3, MnO_x–Pt/La–Al_2O_3, MnO_x–Pd/Al_2O_3, and MnO_x–Pd/La–Al_2O_3) were similar and not well defined; therefore, these will not be discussed here. However, the initial composition of the samples could be determined. After the experiments the samples were green which is the color of bulk MnO. Further reduction to

metallic manganese does not proceed until over 1200°C. The H_2/Mn ratios of the fresh samples, calcined at 800°C, showed values of approximately 0.5, which indicates the presence of mainly Mn_2O_3. Moreover, it is known that between 500–600°C MnO_2 is converted into Mn_2O_3 when calcined in air (42). Therefore, the reduction sequence was probably $Mn_2O_3 \Rightarrow Mn_3O_4 \Rightarrow MnO$ (43, 44). The H_2/Mn ratios of the aged samples at 900°C showed values in the region of 0.33, which indicates a large proportion of Mn_3O_4, that should be formed at this temperature (42).

Copper Oxide Samples

Dumas *et al.* (45) showed that H_2 TPR of CuO/Al_2O_3 may exhibit different reduction peaks. One corresponds to the reduction at 200–220°C of the surface copper species for copper loading under saturation of alumina, i.e., <6.4–8 mol% Cu/100 m^2/g Al_2O_3 (46). According to several authors (46–49), these species in strong interaction with alumina would consist of Cu^{2+} ions, forming on the surface of the alumina, a structure related to that of a spinel compound. Also, Garbowski and Primet (50) reported that Cu^{2+} ions may be anchored by the hydroxyl groups of alumina. It is believed that a "surface spinel" compound is an unusual structure (different from bulk spinel compounds), occupying tetragonal distorted octahedral sites (>90%) with only a small fraction located in the tetrahedral sites (46, 51). Two surface copper species can be distinguished by ESR and magnetic susceptibility: isolated and interacting or clustered ions (52–54). As the copper loading increases, the ratio between the isolated and the interacting species decreased; however, Centi *et al.* reported the latter to be predominant even at very low loading (53). With higher copper loading, segregation of CuO appears. Reduction of CuO appears at a higher temperature (ca. 300°C) than the reduction of surface Cu^{2+} (41, 45), since surface ions are more reactive toward hydrogen (41). Bulk copper aluminate (60% tetrahedral and 40% octahedral Cu^{2+}) can be formed only at high calcination temperatures, i.e., above ca 800°C (34, 46, 49), and is reduced at temperatures of around 500°C (41, 45).

In order to understand the nature of the copper species in this study, some TPR experiments on CuO/Al_2O_3 (1.6 to 8 mol% Cu/100 m^2/g Al_2O_3) were conducted. At 1.6 mol% Cu, the TPR profile showed a single peak at 250°C (Fig. 3). Above 4.8 mol% Cu, a second peak appeared at 250°C and grew with increasing content of copper which also corresponded to the detection of CuO by XRD analyses (data not shown). Furthermore, the color of the samples varied from green to gray with an increasing amount of copper, indicating the progressive formation of CuO. With a larger concentration of copper, the temperature of reduction of the second step increased, indicating that the larger the particle size, the higher is the reduction temperature which tended to be close to that of the bulk CuO.

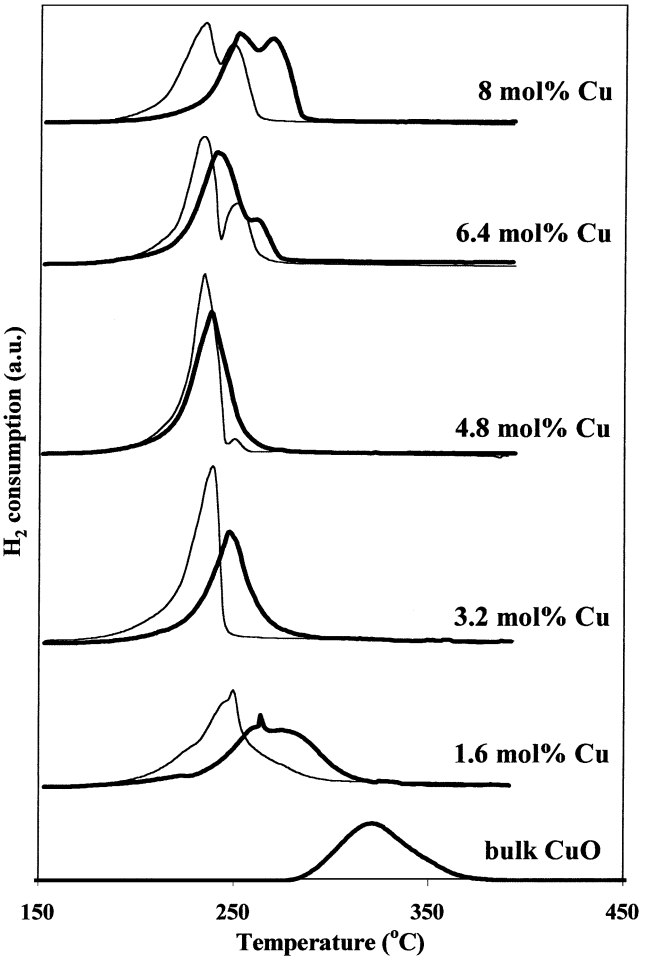

FIG. 3. TPR profiles of bulk CuO and CuO (1.6 to 8 mol% Cu/100 m^2/g Al_2O_3) deposited on alumina alone (thin line) and stabilized with lanthanum (thick line), calcined at 300°C for 4 h.

Fresh Samples

Profiles of the four samples containing copper oxide ($CuO–Pt/Al_2O_3$, $CuO–Pt/La–Al_2O_3$, $CuO–Pd/Al_2O_3$ and $CuO–Pd/La–Al_2O_3$) calcined at 800°C presented a single peak for each (Fig. 4). The H_2/Cu ratio was equal to 1 for all the fresh samples. According to the TPR results above, this meant that all fresh samples contained surface Cu^{2+} on the alumina. Since the copper concentration is fairly high and close to the saturation value, the surface species may consist mostly of clustered ions as described above. Whereas on the fresh catalysts prepared by the deposition–precipitation method, the saturation of alumina with copper was not yet reached at 7.5 mol% Cu/100 m^2/g Al_2O_3, the copper catalysts prepared by the incipient wetness technique showed saturation between 3.2 and 4.8 mol% Cu/100 m^2/g Al_2O_3 (Fig. 3). This means that the saturation of alumina with copper can be extended by using an appropriate preparation method.

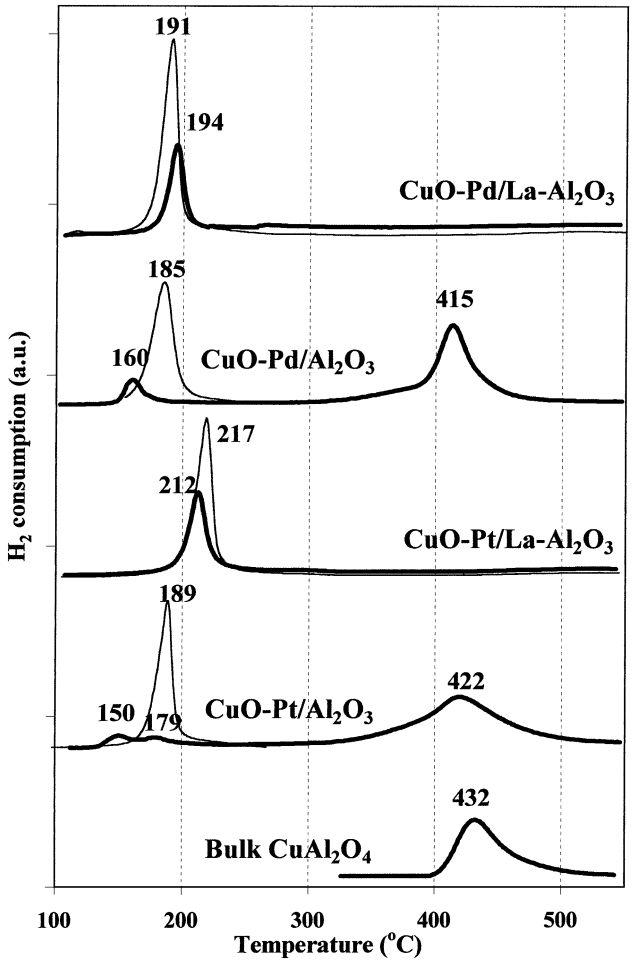

FIG. 4. TPR profiles of bulk $CuAl_2O_4$, CuO–Pt, and CuO–Pd (Cu, 10 mol%/Al_2O_3; Pt, Pd, 0.1 mol%/Al_2O_3) deposited on alumina alone and stabilized with lanthanum (3 mol% Al_2O_3) calcined at 800°C for 4 h (thin line) and after hydrothermal treatment at 900°C for 300 h in 10% steam (thick line).

Copper-based samples containing Pd presented a lower reduction peak temperature compared to samples with Pt. The effect of noble metals on the reduction temperature of metal oxides has already been reported (37, 55) with Pd having a stronger effect than Pt as observed in a previous study (56). The presence of group VIII metals promotes the reduction of metal oxide. Gentry *et al.* (55) studied the effect of various amounts of Pt and Pd on the reduction of unsupported copper oxide. They proposed the following mechanism: Hydrogen is dissociatively adsorbed on metal islands of Pd and Pt which is then transferred by a spillover process to CuO, which then is easily reduced. According to Gentry *et al.* (55), the fact that Pd has a stronger effect on the reduction of CuO compared to Pt is due to the ability of Pd^{2+} to substitute Cu^{2+} within the CuO lattice without phase separation.

Fresh samples containing lanthanum had a higher reduction peak temperature compared to those without lanthanum (Fig. 4). This effect was particularly stronger for Pt, probably because Pd, compared to Pt, favored the reduction of CuO. The slight differences in surface areas and pore size distribution between doped and undoped fresh samples were unlikely to be the causes of the divergence. It seems more likely that the temperature at which the reduction occurs depends mostly on the strength of the interactions between the metal and the support (38). In order to compare the influence of the support on the reduction of CuO, TPR experiments on CuO/La–Al_2O_3 (from 1.6 to 8 mol% Cu/100 m^2/g Al_2O_3) were performed (Fig. 3). The results showed that, for each copper content, the reduction of copper oxide on doped alumina occurred at a higher temperature than that with alumina alone. This could be a consequence of stonger interactions between copper and alumina, as the support was less crystalline in the presence of lanthanum. Indeed, Solcova *et al.* (39) found that more crystalline supports helped increase the reducibility of NiO due to weaker interactions between NiO and the support, as compared to that on amorphous support (57, 58). In the present study, the formation of CuO appeared at a copper concentration of 4.8–6.4 mol% for the sample containing lanthanum, whereas in the case of alumina alone, CuO was already detectable at a concentration of 3.2–4.8 mol%. This indicates that lanthanum increased the dispersion of copper onto alumina, thus leading to a higher saturation value of copper within the alumina. For samples without lanthanum, the width of the peaks was larger, particularly for CuO–Pd. This means that the presence of lanthanum brought about a better dispersion of the copper species.

Hydrothermally Treated Samples

After aging, the profiles of CuO–Pt/Al_2O_3 presented three peaks, i.e., two at low temperatures (150°C and 179°C) having approximately equal areas, and a larger peak at a higher temperature (422°C). For CuO–Pd/Al_2O_3, there were only two peaks: a small one at low temperature (160°C) and a larger one at a higher temperature (415°C), as seen in Fig. 4. The H_2/Cu ratio was equal to 1 for all the hydrothermally treated samples.

According to the reduction profile of a reference $CuAl_2O_4$ sample showing a single peak at 432°C, the peak at high temperature corresponds to the presence of bulk spinel compounds. This was also confirmed by XRD measurements. According to the hydrogen consumption corresponding to this peak, ca. 64 and 81% of the initial copper had reacted with alumina to form bulk aluminate in CuO–Pt and CuO–Pd, respectively. The hydrogen consumption in the second step for both CuO–Pt and CuO–Pd samples was proportionally related to the XRD intensities of $CuAl_2O_4$ in these samples. Hence, $CuAl_2O_4$ would seem to be the major species after hydrothermal treatment. The stronger spillover effect of Pd compared to Pt on the reduction of

copper species, as mentioned above, is clearly seen on the reduction of copper aluminate.

The small thermoreduction peaks at lower temperature, compared to those of fresh samples, can be ascribed to an increase in reducibility of the copper species, as described above. Therefore, the shift of the peak toward a lower temperature is attributed to the decrease of interactions between CuO and Al_2O_3, which became more crystalline after the treatment. This was also confirmed by the lower reduction temperature of the first peak for the CuO–Pd sample which, according to XRD, also presented a higher amount of the α phase compared to CuO–Pt. For the CuO–Pt sample, the two peaks at low temperatures could be attributed to surface Cu^{2+} and to CuO crystallites, as explained above. For the CuO–Pd sample, the presence of a single peak at low temperatures could be due to the reduction of the main species, CuO. Indeed, the alumina washcoat in this sample was composed of ca. 80% α-alumina phase, which has a hexagonal close-packed structure that cannot allow for copper ions to be in a defective spinel structure such as γ-alumina.

Hydrothermally treated samples stabilized with lanthanum exhibited single peaks at approximately the same reduction temperature as for the fresh samples (Fig. 4). This means that surface Cu^{2+} on the alumina was still present, as seen by the single thermoreduction peak. No bulk spinel compounds were found here. A low but constant consumption of hydrogen toward high reduction temperatures was observed, especially for CuO–Pd/La–Al_2O_3, showing the presence of hardly reducible species, due probably to a diffusion of Cu^{2+} ions into the support with increasing calcination temperature (46, 48).

X-Ray Photoelectron Spectroscopy

Table 2 shows the values of the binding energies (BEs) for La $3d_{5/2}$, Mn $2p_{3/2}$, and Cu $2p_{3/2}$, as well as the atomic ratios of La/Al, Mn/Al, and Cu/Al for the samples of Al_2O_3, La–Al_2O_3, MnO_x–Pt, and CuO–Pt deposited on undoped or doped alumina, before and after hydrothermal treatment. The data of other compounds, viz. La_2O_3, $LaAlO_3$, $La(OH)_3$, dispersed "La" phase, MnO_2, Mn_2O_3, Mn_3O_4, MnO, $MnAl_2O_4$, Cu^o, Cu_2O, CuO, and $CuAl_2O_4$, obtained in different studies, have been corrected, referenced to C 1*s* at 284.6 eV, and summarized in Table 3.

The La $3d_{5/2}$ BE values for all samples, fresh and aged, containing lanthanum were similar and equal to 835.3–835.7 eV, which are substantially higher than the values observed for La_2O_3 or $LaAlO_3$ standards (59–62), but close to the values found for dispersed "La" phase (Table 3). Some authors rejected the fact that the high BE can be attributed to the nature of the support or to the particle size effect (59, 60). In this study, the concentration value of ca. 2 μmol La/m^2 is far lower than the saturation concentration for dispersed lanthanum in γ-alumina determined in the literature, which varies between ca. 8.5 and 60 μmol La/m^2 (21, 59, 63, 64). According to Bettman, under saturation concentration, lanthanum is in a two-dimensional dispersed phase (63).

The BEs of the principal Mn $2p_{3/2}$ peak for all the samples containing the mixture of manganese oxides and Pt were between 641.5 and 641.7 eV (Table 2), which may correspond to the presence of mainly Mn_2O_3, as determined on fresh samples according to TPR results; however, on aged samples Mn_3O_4 was found. There is respectively a complete and large overlapping of the Mn $2p_{3/2}$ peak position domain between MnO_2 and Mn_2O_3 on the one hand and Mn_2O_3 and Mn_3O_4 on the other hand (65). Therefore, the determination of the manganese oxidation state on the basis of the Mn $2p_{3/2}$ peak position is difficult. There was no indication that $MnAl_2O_4$ existed in our samples. It has been reported that the formation of $MnAl_2O_4$ occurs only when samples are calcined in reducing atmosphere, because of the instability of Mn^{2+} ions in air at temperatures above 150°C (44, 47, 66).

TABLE 2

Data from XPS Analysis of Catalysts Calcined at 800°C for 4 h in Air (Fresh) and Hydrothermally Treated at 900°C for 300 h in 10% Steam (HT) (La, 3 mol%/Al_2O_3; Mn, Cu, 10 mol% Al_2O_3; Pt, Pd, 0.1 mol%/Al_2O_3)

	Binding energies (eV)[a]			Atomic ratios		
	La $3d_{5/2}$	Mn $2p_{3/2}$	Cu $2p_{3/2}$	La/Al	Mn/Al	Cu/Al
La–Al_2O_3, Fresh	835.4 (6.0)			0.024		
La–Al_2O_3, HT	835.4 (5.1)			0.013		
MnO_x–Pt/Al_2O_3, Fresh		641.6 (4.3)			0.078	
MnO_x–Pt/Al_2O_3, HT		641.7 (3.9)			0.15	
MnO_x–Pt/La–Al_2O_3, Fresh	835.7 (6.2)	641.7 (4.1)		0.034	0.13	
MnO_x–Pt/La–Al_2O_3, HT	835.3 (6.4)	641.5 (4.1)		0.024	0.12	
CuO–Pt/Al_2O_3, Fresh			933.4 (3.6)			0.13
CuO–Pt/Al_2O_3, HT			933.6 (3.7)			0.23
CuO–Pt/La–Al_2O_3, Fresh	835.3 (6.0)		932.8 (3.2)	0.016		0.13
CuO–Pt/La–Al_2O_3, HT	835.4 (6.1)		933.2 (3.4)	0.021		0.12

[a] All BEs (eV) referenced to C 1*s* = 284.6 eV. Values in parentheses are full width at half-maximum (FWHM).

TABLE 3

Binding Energies (eV) of Reference Compounds

	Binding energies (eV)[a]			
	La $3d_{5/2}$	Mn $2p_{3/2}$	Cu $2p_{3/2}$	Ref.
La_2O_3	833.2			(59)
	833.5			(60)
	833.8			(61)
$LaAlO_3$	833.8			(59)
	835.7			(60)
$La(OH)_3$	834.8			(61)
Dispersed "La"	835.0			(59, 62)
	835.5			(61)
	836.1			(60)
MnO_2		641.7		(70)
		642.1		(44)
		642.2		(70, 65)
Mn_2O_3		641.4		(44, 65)
		641.5		(71)
Mn_3O_4		640.9		(44)
		641.1		(71)
MnO		640.1		(70)
		640.6		(71)
		641.2		(44)
$MnAl_2O_4$		641.1		(44)
Cu°			932.0	(72)
Cu_2O			932.1	(48, 72)
CuO			933.6	(46, 48)
			933.7	(72)
			933.9	(54, 73)
$CuAl_2O_4$			934.5	(48)
			934.6	(46)
			934.8	(73)
			935.0	(54)

[a] All BEs (eV) referenced to C ls = 284.6 eV.

The BE of the principal Cu $2p_{3/2}$ peak, for the samples containing a mixture of copper oxides and Pt, was lower than the values usually found for CuO (Tables 2 and 3), except for the hydrothermally treated CuO–Pt/Al_2O_3, which had the highest BE (933.6 eV). According to TPR data, bulk CuO was also detected only on aged CuO–Pt/Al_2O_3. This means that for fresh samples of CuO–Pt/Al_2O_3 and for the fresh and aged samples of CuO–Pt/La–Al_2O_3, the copper species were different from bulk CuO. It must be noted that although the observed BEs for samples may be close to those of bulk compounds, it does not mean that these compounds are necessarily present on the catalyst surface (48). In all spectra obtained, a satellite in the high BE side of Cu $2p_{3/2}$ could be seen, which is characteristic of the presence of Cu^{2+} (67–69). However, Cu^{2+} can be in the form of CuO or $CuAl_2O_4$. According to Strohmeier *et al.*, CuO and $CuAl_2O_4$ can be distinguished by comparison of their satellite intensity to that of the main photoelectron line which was 1.10 for $CuAl_2O_4$ and 0.45 for CuO (48). Hence, since the Cu $2p_{3/2}$ BE of the catalysts gave little information, the satellite intensities (relative to the main Cu $2p_{3/2}$ photoelectron line) were determined to indicate which species were present on the catalysts. A ratio of ca. 0.42 was found for the hydrothermally treated CuO–Pt/Al_2O_3, while lower ratios were found for the fresh samples of CuO–Pt/Al_2O_3 and for the fresh and aged samples of CuO–Pt/La–Al_2O_3. This meant that bulk CuO was present only in the hydrothermally treated CuO–Pt/Al_2O_3, as confirmed by TPR. It is likely that the surface of the aged CuO–Pt/Al_2O_3 sample was covered by a layer of CuO, which could explain why bulk copper aluminate could not be detected by XPS.

The theoretical value of the Me/Al (Me = Mn, Cu) ratio is equal to 0.05. However, the ratios measured for the fresh samples were higher than that (Table 2). This could be due to a surface enrichment or smaller particles at the same surface concentration. The addition of lanthanum had a small effect on the dispersion of copper in fresh samples, whereas for fresh manganese samples, the measured Mn/Al ratio was higher in the presence of lanthanum. This indicates that lanthanum increased the dispersion of manganese oxides, or that manganese particles were smaller in the presence of lanthanum. This can be attributed to interactions between lanthanum and manganese oxides during insertion of the manganese salt. Indeed, the La/Al atomic ratio increased following the deposition of manganese, which suggests that lanthanum phases dissolved in the solution containing manganese salt. However, after hydrothermal treatment at 900°C for 300 h, the samples deposited on alumina alone become enriched in Mn and Cu at the surface as shown by an increasing Me/Al ratio, whereas, for the MnO_x–Pt/La–Al_2O_3 and CuO–Pt/La–Al_2O_3 samples, the Me/Al ratios were similar to those of the fresh samples. This could be explained by the fact that lanthanum stabilizes the washcoat and the dispersion of the metal oxides and prevents coalescence of particles after hydrothermal treatment. The increase of the Me/Al ratio was higher in the case of CuO–Pt, compared to MnO_x–Pt, probably because of the higher extent of sintering in the copper samples, as observed by XRD. The differences in surface compositions obtained by EDX (HRTEM section) and by XPS (Table 2) can be explained by the larger analysis depth of EDX compared to XPS.

Metal–Support Interactions

The results from the characterization studies showed that the presence of metal oxides and noble metals in the washcoat increased the effects of sintering of the catalysts, viz. decrease of the BET surface area, transformation of γ- to α-alumina phases at lower temperatures, increase of the alumina particle size, and stronger interactions of the active phases with alumina. In general terms, the role of foreign ions is easy to explain. Thermal reorganization involves diffusion via defects and vacancies (2). The presence of both metal oxides accelerated the sintering, with copper oxide having a stronger effect than manganese

oxides. In this study, after calcination at 800°C, Cu^{2+} was found to be present on samples containing copper and Mn_2O_3 was present in the samples containing manganese. According to many authors, many transition metals acted as accelerators for the transformation of γ- to α-alumina phases (2, 10, 11). The size of the ionic radii and the charge also play an important role in the mobility of the ion into the alumina. A larger charge and ionic radius favors lower mobility (6, 11, 16). The ionic radii of these metal ions are 0.72 Å and 0.66 Å for Cu(+II) and Mn(+III), respectively (74). According to the model described by Burtin *et al.* (75), which takes into account charge and ionic radius, it seems that Cu(+II) has a more pronounced effect as an accelerator than Mn(+III) does. That could explain the higher mobility of copper in the alumina structure compared to manganese, leading to the higher extent of alumina sintering. Lanthanum ions introduced into the alumina structure decreased the solubility of copper and manganese ions, thus restraining the interaction between Cu and Mn with alumina, and reducing the catalyst's sintering. Lanthanum ions, by covering a large fraction of the alumina surface, may also hinder the reaction between the active phases and alumina and restrain the hydroxylation of the support that favors sintering and aggregation.

Catalytic Activities

In the present study, for both the fresh manganese- and copper-based catalysts (calcined at 800°C), the presence of lanthanum did not influence the activity for the conversion of $C_{10}H_8$ and CO (Table 4). This is probably due to the fact that lanthanum affects the dispersion of metal oxides more than noble metals, the latter being the "active phases" for the oxidation of CO and $C_{10}H_8$ (29). However, for the oxidation of CH_4, the addition of lanthanum increased the activity for both MnO_x–Pd and MnO_x–Pt catalysts of ca. 20°C at 50% conversion (Table 4). This enhancement in activity for CH_4 oxidation can be explained by a better dispersion of manganese in the presence of lanthanum, as determined by XPS, since manganese oxides are more active than Pt or Pd alone for CH_4 oxidation in the concentration used in the study (29). For the copper-based catalysts, surface copper species were found in all fresh samples (doped and undoped) according to TPR and XPS, thus leading to no significant difference in activity between the doped and undoped catalysts. These isolated Cu^{2+} species were reported to be the active species for the oxidation of CH_4 (36, 41). The CuO–Pd (on Al_2O_3 and La–Al_2O_3) catalysts had the best activity for the oxidation of the combustibles studied here, followed by the CuO–Pt, MnO_x–Pd, and MnO_x–Pt catalysts.

After hydrothermal treatment at 900°C for 300 h in the presence of 10% steam, the activity of the catalysts containing lanthanum were better, particularly for the oxidation of CH_4 (Table 4). The stabilization effect of lanthanum is clearly seen by an example in Fig. 5. The decrease in activity for the oxidation of CH_4 was higher for the catalysts containing copper oxide compared to those with manganese oxides, especially the ones without stabilizer. This may be the result of several reasons. First, according to the results from the characterization studies, copper led to a higher extent of alumina sintering compared to manganese. Furthermore, in the copper samples, the formation of copper aluminate may have contributed to the decrease of oxidation. Indeed, copper in $CuAl_2O_4$ does not possess the ability to change oxidation state, but remains as Cu(+II). Thus, copper cannot be an active redox center for oxidation of VOCs which generally proceed via the Mars–van Krevelen type of mechanism (i.e., redox mechanism) (76). In addition, for all the catalysts containing manganese oxides, Mn_3O_4 was found to be present, as observed by TPR on the fresh samples; these are more active for the oxidation of some hydrocarbons than Mn_2O_3 (12, 77). However, in this study, no enhancement in activity was seen for the manganese oxide catalysts, probably because of the high loss of surface area. The CuO–Pd/La–Al_2O_3 catalyst was

TABLE 4

Temperature (°C) for 50% Conversion Carbon Monoxide, Naphthalene, and Methane for Catalysts Calcined at 800°C for 4 h in Air (Fresh) and Hydrothermally Treated at 900°C for 300 h in 10% steam (HT) (La, 3 mol%/Al_2O_3; Mn, Cu, 10 mol%/Al_2O_3; Pt, Pd, 0.1 mol%/Al_2O_3)

	CO			$C_{10}H_8$			CH_4		
	Fresh	HT	ΔT^a	Fresh	HT	ΔT^a	Fresh	HT	ΔT^a
MnO_x–Pt/Al_2O_3	290	330	40	287	320	33	639	706	67
MnO_x–Pt/La–Al_2O_3	288	327	39	284	316	32	620	688	68
MnO_x–Pd/Al_2O_3	283	342	59	284	332	48	636	716	80
MnO_x–Pd/La–Al_2O_3	287	310	23	287	314	27	618	674	56
CuO–Pt/Al_2O_3	266	284	18	271	289	18	602	724	122
CuO–Pt/La–Al_2O_3	266	276	10	273	281	8	599	686	87
CuO–Pd/Al_2O_3	216	392	176	221	406	185	578	748	170
CuO–Pd/La–Al_2O_3	214	259	45	221	268	47	577	652	75

[a] $\Delta T = T_{50}(\text{HT}) - T_{50}(\text{fresh})$.

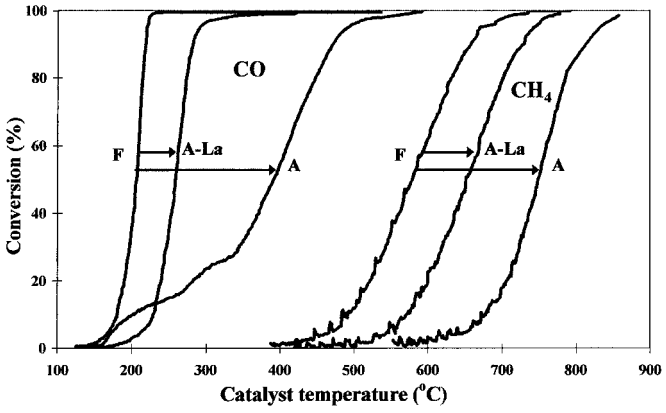

FIG. 5. Conversion of CO and CH_4 over CuO–Pd (Cu, 10 mol%/Al_2O_3; Pd, 0.1 mol%/Al_2O_3) catalysts deposited on alumina alone and stabilized with lanthanum (3 mol%/Al_2O_3) calcined at 800°C for 4 h (F) and after hydrothermal treatment at 900°C for 300 h in 10% steam (A). CuO–Pd/Al_2O_3 (fresh, F; aged, A), CuO–Pd/La–Al_2O_3 (fresh, F; aged, A-La).

still the best catalyst for the oxidation of CO, $C_{10}H_8$, and CH_4 after hydrothermal treatment.

CONCLUSIONS

In conclusion, the presence of lanthanum in the alumina serves to stabilize the latter, thus allowing it to retain high surface area and its amorphous structure under high-temperature conditions, such as those found during wood combustion. This lanthanum stabilization of the alumina structure extends to a better dispersion and a higher saturation of the metal oxides onto the support, while at the same time stabilizing the oxidation activity of these catalysts by preventing the interaction of metal oxide with alumina to form inactive bulk spinel compounds. Under the experimental conditions of this study, CuO–Pd/La–Al_2O_3 catalyst was found to be the best for the oxidation of CO, $C_{10}H_8$, and CH_4 before and after hydrothermal treatment at 900°C for 300 h in 10% steam. Since methane is one of the most problematic compounds released in the combustion of wood, the application of such stabilized washcoat supports would be very useful to the long-term and cost-effective utilization of mixed metal oxides and noble metals catalysts for the removal of this gas, as well as of other VOCs, under high-temperature conditions.

ACKNOWLEDGMENTS

This work was financed by the Swedish National Energy Administration (STEM), by NUTEK (which is the Swedish National Board for Industrial and Technical Development), and by the European Commission, the FAIR program, CT95-0682. Thanks are given to Michel Bellais for the preparation of catalysts and to Inga Groth for help with the SEM at the Division of Chemical Technology, the Royal Institute of Technology. We also thank Hans Bergqvist (Division of Materials Science and Engineering, the Royal Institute of Technology) for the TEM analyses, Gabrielle Ehret (Institut de Physique et de Chimie des Matériaux de Strasbourg, France) for the HRTEM analyses, and Lars T. Andersson (University of Lund) for the XPS analyses.

REFERENCES

1. Carol, L. A., Newman, N. E., and Mann, G. S., SAE Paper 892040.
2. Trimm, D. L., *in* "Catalyst Deactivation" (C. H. Bartholomew and J. B. Butt, Eds.), p. 29. Elsevier, Amsterdam, 1991.
3. Shkrabina, R. A., Koryabkina, N. A., Kirichenko, O. A., Ushakov, V. A., Kapteijn, F., and Ismagilov, Z. R., *in* "Preparation of Catalysts VI" (G. Poncelet *et al.*, Eds.), p. 1145. Elsevier, Amsterdam, 1995.
4. Nortier, P., and Soustelle, M., *in* "Catalysis and Automotive Pollution Control" (A. Crucq and A. Frennet, Eds.), Stud. Surf. Sci. Catal., p. 275. Elsevier, Amsterdam, 1987.
5. Tucci, E. R., *Hydrocarbon Processing* 159 (1982).
6. Miyoshi, N., Matsumoto, S., Ozawa, M., and Kimura, M., SAE Paper 891970.
7. Dalla Betta, R. A., McCune, R. C., and Sprys, J. W., *Ind. Eng. Chem., Prod. Res. Dev.* **15**(3), 169 (1976).
8. Chu, Y. F., and Ruckenstein, E., *J. Catal.* **55**, 281 (1978).
9. Kozlov, N. S., Lazarev, M. Ya., Mostovaya, L. Ya., and Stremok, I. P., *Kinet. Katal.* **14**(5), 1287 (1973) (in Russian).
10. Vereschagin, V. I., Zelinskii, V. Yu., Khabas, T. A., and Kolova, N. N., *J. Appl. Chem. USSR* **55**(9), 1946 (1982).
11. Burtin, P., Brunelle, J. P., Pijolat, M., and Soustelle, M., *Appl. Catal.* **34**, 225 (1987).
12. Ferrandon, M., Berg, M., and Björnbom, E., *Catal. Today* **53**, 647 (1999).
13. Young, D. J., Udaja, P., and Trimm, D. L., *in* "Catalyst Deactivation" (B. Delmon and G. F. Froment, Eds.), p. 331. Elsevier, Amsterdam, 1980.
14. Ozawa, M., Toda, H., Kato, O., and Suzuki, S., *Appl. Catal. B* **8**, 123 (1996).
15. Peiyan, L., Weidong, C., and Shouming, Y., *J. Mol. Catal. (China)* **9**(3), 179 (1995).
16. Church, J. S., Cant, N. W., and Trimm, D. L., *Appl. Catal.* **101**, 105 (1993).
17. Ozawa, M., Toda, H., Kato, O., and Suzuki, S., *Appl. Catal. B* **8**, 141 (1996).
18. Béguin, B., Garbowski, E., and Primet, M., *Appl. Catal.* **75**, 119 (1991).
19. Schaper, H., Amesz, D. J., Doesburg, E. B. M., and Van Reijen, L. L., *Appl. Catal.* **9**, 129 (1984).
20. Oudet, F., Bordes, E., Courtine, P., Maxant, G., Lambert, C., and Guerlet, J. P., *in* "Catalysis and Automotive Pollution Control" (A. Crucq and A. Frennet, Eds.), Stud. Surf. Sci. Catal., Vol. 30, p. 313. Elsevier, Amsterdam, 1987.
21. Jun-Ying, Y., and Swartz, Jr, W. E., *Spectrosc. Lett.* **17** (6–7), 331 (1984).
22. Härkönen, M. A., Aitta, E., Lahti, A., Luoma, M., and Maunula, T., SAE Paper 910846.
23. Chou, T. Y., Leu, C. H., and Yeh, C. T., *Catal. Today* **26**, 53 (1995).
24. Oudet, F., Vejux, A., and Courtine, P., *Appl. Catal.* **50**, 79 (1989).
25. Schaper, H., Doesburg, E. B. M., and Van Reijen, L. L., *Appl. Catal.* **7**, 211 (1983).
26. Matsuda, S., Kato, A., Mizumoto, M., and Yamashita, H., "Proceedings, 8th International Congresson Catalysis, Berlin, 1984," Vol. IV, p. 879. Dechema, Frankfurt-am-main, 1984.
27. Tijburg, I. I. M., Geus, J. W., and Zandbergen, H. W., *J. Mater. Sci.* **26**, 6479 (1991).
28. Mizukami, F., Maeda, K., Watanabe, M., Masuda, K., Sano, T., and Kuno, K., *in* "Catalysis and Automotive Pollution Control II" (A. Crucq, Ed.), Stud. Surf. Sci. Catal., p. 557. Elsevier, Amsterdam, 1991.
29. Ferrandon, M., Carnö, J., Järås, S., and Björnbom, E., *Appl. Catal. A* **180**, 153 (1999).

30. Geus, J. W., *in* "Preparation of Catalysts III" (G. Poncelet, P. Grange, and P. A. Jacobs, Eds.), p. 1. Elsevier, Amsterdam, 1983.
31. Farrauto, J., and Hobson, M., *Encyclopedia Phys. Sci. Technol.* **2**, 735 (1992).
32. Monti, D. A. M., and Baiker, A., *J. Catal.* **83**, 323 (1983).
33. Wallbank, B., Johnson, C. E., and Main, I. G., *J. Electron Spectrosc.* **4**, 263 (1974).
34. Misra, S. K., and Chaklader, A. C. D., *J. Am. Ceram. Soc.* **46**(10), 509 (1963).
35. Ranganathan, T., MacKean, B. E., and Muan, A., *J. Am. Ceram. Soc.* **45**(6), 280 (1962).
36. Jiang, X. y., Zhou, R. x., Pan, P., Zhu, B., Yuan, X. x., and Zheng, X. m., *Appl. Catal. A* **150**, 131 (1997).
37. Hurst, N. W., Gentry, S. J., and Jones, A., *Catal. Rev.-Sci. Eng.* **24**(2), 233 (1982).
38. Gentry, S. J., and Walsh, P. T., *J. Chem. Soc., Faraday Trans. I* **78**, 1515 (1982).
39. Solcova, O., Uecker, D. C., Steinike, U., and Jiratova, K., *Appl. Catal. A* **94**, 153 (1993).
40. Severino, F., Brito, J., Carías, O., and Laine, J., *J. Catal.* **102**, 172 (1986).
41. Marion, M. C., Garbowski, E., and Primet, M., *J. Chem. Soc, Faraday Trans.* **87**(11), 1795 (1991).
42. Reidies, A. H., *in* "Ullmann's Encyclopedia of Industrial Chemistry" (B. Elvers, S. Hawkins, and G. Schulz, Eds.), 5th Ed., Vol. A16, p. 123. VCH, New York, 1986.
43. Kapteijn, F., van Langeveld, A. D., Moulijn, J. A., Andreöni, A., Vuurman, M. A., Turek, A. M., Jehng, J.-M., and Wachs, I. E., *J. Catal.* **150**, 94 (1994).
44. Strohmeier, B. R., and Hercules, D. M., *J. Phys. Chem.* **88**, 4922 (1984).
45. Dumas, J. M., Geron, C., Kribii, A., and Barbier, J., *Appl. Catal.* **47**, L9 (1989).
46. Friedman, R. M., Freeman, J. J., and Lytle, F. W., *J. Catal.* **55**, 10 (1978).
47. Lo Jacono, M., and Schiavello, M., *in* "Preparation of Catalysts" (B. Delmon, P. A. Jacobs, and G. Poncelet, Eds.), p. 473. Elsevier, Amsterdam, 1976.
48. Strohmeier, B. R., Leyden, D. E., Field, R. S., and Hercules, D. M., *J. Catal.* **94**, 514 (1985).
49. Wolberg, A., and Roth, J. F., *J. Catal.* **15**, 250 (1969).
50. Garbowski, E., and Primet, M., *J. Chem. Soc., Chem. Commun.* 11 (1991).
51. Freeman, J. J., and Friedman, R. M., *J. Chem. Soc., Faraday Trans. 1* 758 (1978).
52. Berger, P. A., and Roth, J. F., *J. Phys. Chem.* **71**(13), 4307 (1967).
53. Centi, G., Perathoner, S., Biglino, D., and Giamello, E., *J. Catal.* **151**, 75 (1995).
54. Park, P. W., and Ledford, J. S., *Appl. Catal. B* **15**, 221 (1998).
55. Gentry, S. J., Hurst, N. W., and Jones, A., *J. Chem. Soc., Faraday Trans. 1* **77**, 603 (1981).
56. Ferrandon, M., Carnö, J., Jörås, S., and Björnbom, E., *Appl. Catal. A* **180**, 141 (1999).
57. Mile, B., Stirling, D., Zammitt, M. A., Lovell, A., and Webb, M., *J. Catal.* **114**, 217 (1988).
58. Kadkhodayan, A., and Brenner, A., *J. Catal.* **117**, 311 (1989).
59. Haack, L. P., de Vries, J. E., Otto, K., and Chattha, M. S., *Appl. Catal. A* **82**, 199 (1992).
60. Ledford, J. S., Houalla, M., Proctor, A., Hercules, D. M., and Petrakis, L., *J. Phys. Chem.* **93**(18), 6770 (1989).
61. Alvero, R., Bernal, A., Carrizosa, I., and Odriozola, J. A., *Inorg. Chim. Acta* **140**, 45 (1987).
62. Talo, A., Lahtinen, J., and Hautojärvi, P., *Appl. Catal. B* **5**, 221 (1995).
63. Bettman, M., Chase, R. E., Otto, K., and Weber, W. H., *J. Catal.* **117**, 447 (1989).
64. Scheithauer, M., Knözinger, H., and Vannice, M. A., *J. Catal.* **178**, 701 (1998).
65. Wagner, C. D., Riggs, W. M., Davis, L. E., and Moulder, J. F., *in* "Handbook of X-ray Photoelectron Spectroscopy" (G. E. Muilenberg, Ed.). Perkin-Elmer, Eden Prairie, MN, 1979.
66. Wang, W., Yang, Y., and Zhang, J., *Appl. Catal. A* **131**, 189 (1995).
67. Fiermans, L., Hoogewijs, R., and Vennik, J., *Surf. Sci.* **47**, 1 (1975).
68. Scrocco, M., *Chem. Phys. Lett.* **63**(1), 52 (1979).
69. Rosencwaig, A., and Wertheim, G. K., *J. Electron. Spectrosc. Relat. Phenom.* **1**, 493 (1972).
70. Baltanás, M. A., Katzer, J. R., and Stiles, A. B., *Acta Chim. Hung.* **124**(3), 341 (1987).
71. Di Castro, V., and Polzonetti, G., *J. Electron. Spectrosc. Relat. Phenom.* **48**, 117 (1989).
72. Ertl, G., Hierl, R., Knözinger, H., Thiele, N., and Urbach, H. P., *Appl. Surf. Sci.* **5**, 49 (1980).
73. Wolberg, A., Ogilvie, J. L., and Roth, J. F., *J. Catal.* **19**, 86 (1970).
74. Weast, R. C., and Astle, M. J., "Handbook of Chemistry and Physics," 59th Ed. CRC Press, Boca Raton, FL, 1979.
75. Burtin, P., Brunelle, J. P., Pijolat, M., and Soustelle, M., *Appl. Catal.* **34**, 239 (1987).
76. Spivey, J. J., *in* "Complete Catalytic Oxidation of Volatile Organics" (G. C. Bond and G. Webb, Eds.), Catalysis, Vol. 8. The Royal Soc. Chem. Cambridge, 1989.
77. Tsyrul'nikov, P. G., Kovalenko, O. N., Gogin, L. L., Starostina, T. G., Noskov, A. S., Kalinkin, A. V., Krukova, G. N., Tsybulya, S. V., Kudrya, E. N., and Bubnov, A. V., *Appl. Catal. A* **167**, 31 (1998).